Available online at www.sciencedirect.com
ScienceDirect
ELSEVIER
Applied Surface Science xxx (2007) xxx–xxx
applied surface science
www.elsevier.com/locate/apsusc

Nonlinear optical properties of Au/ZnO nanoparticle arrays

Tingyin Ning, Yueliang Zhou *, Hong Shen, Heng Lu, Zhihui Sun, Lingzhu Cao, Dongyi Guan, Dongxiang Zhang, Guozhen Yang

Institute of Physics, Chinese Academy of Sciences, P.O. Box 603, Beijing 100080, China

Received 3 July 2007; received in revised form 27 July 2007; accepted 27 July 2007

Abstract

The triangular-shaped Au/ZnO nanoparticle arrays were fabricated on fused quartz substrate using nanosphere lithography. The structural characterization of the Au/ZnO nanoparticle arrays was investigated by atomic force microscopy. The absorption peak due to the surface plasmon resonance of Au particles at the wavelength of about 570 nm was observed. The nonlinear optical properties of the nanoparticle arrays were measured using the *z*-scan method at a wavelength of 532 nm with pulse duration of 10 ns. The real and imaginary part of third-order nonlinear optical susceptibility, Re $\chi^{(3)}$ and Im $\chi^{(3)}$, were determined to be 1.15×10^{-6} and -5.36×10^{-7} esu, respectively. The results show that the Au/ZnO nanoparticle arrays have great potential for future optical devices.

PACS : 42.70.−a; 61.46.−w; 78.67.−n; 81.07.−b

Keywords: Nanoparticle arrays; Optical nonlinearity; Nanosphere lithography; *z*-Scan

1. Introduction

Nanoparticles of noble metals (e.g., Ag, Au, Cu) embedded in dielectric matrices have been widely investigated for many years because of their large third-order nonlinear optical susceptibility and fast response time, which are essential for future optical device applications, such as optical switches, optical phase conjugation, and optical computing [1–3]. The greatly enhanced optical nonlinearity in the nanocomposite materials was known to stem from the giant amplification of the local electric field near and inside the metal particles at the surface plasmon resonance (SPR) frequency [1]. Composite films with different dielectric matrices and metal doping have been reported in recent years [4–7]. Usually, the metal clusters are spherical shaped and randomly dispersed inside the composite materials.

Theoretical studies indicated that the anisotropy of both the shape and geometric distribution of the metal nanoparticles could greatly enhance the third-order nonlinear optical susceptibility $\chi^{(3)}$ as well as figure of merit, $\chi^{(3)}/\alpha$ (α is the absorption coefficient) [8,9]. Experimental investigations, for example, Au/SiO_2 multilayer composite films with nonspherical Au particles and Ag/$BaTiO_3$ composite films consisting of oriented Ag clusters, confirmed the enhancement of $\chi^{(3)}$ and $\chi^{(3)}/\alpha$ via geometric anisotropy [10,11]. Additionally, nanosphere lithography (NSL) as a low-cost, simple but effective technique was widely used to produce nanostructures with anisotropy characters [12]. The optical nonlinearity of gold nanoparticle arrays fabricated using NSL has been reported recently, and a pronounced improvement of $\chi^{(3)}$ and $\chi^{(3)}/\alpha$ were observed compared with that of ultra-thin Au film consisting of randomly distributed spheroidal clusters [13,14]. It is predictable that the optical nonlinearity could be further enhanced if Au nanoparticle arrays were embedded in dielectric matrix with larger dielectric constant and optical nonlinearity. In this paper, we studied the large nonlinear optical response of Au/ZnO nanoparicle arrays fabricated using NSL.

2. Experimental

The Au/ZnO nanoparticle arrays were fabricated using NSL by two steps. First, polystyrene nanospheres with diameters of 200 nm were used to form the single-layer masks on the fused quartz substrates (10 mm × 10 mm × 0.5 mm). By dropping

* Corresponding author.
E-mail address: ylzhou@aphy.iphy.ac.cn (Y. Zhou).

0169-4332/$ – see front matter © 2007 Published by Elsevier B.V.
doi:10.1016/j.apsusc.2007.07.195

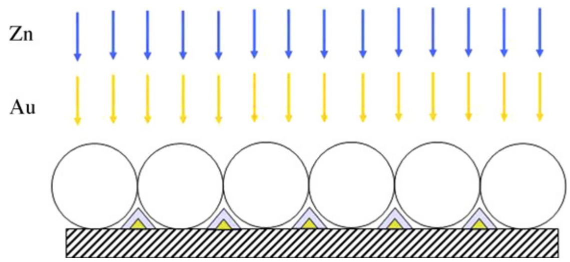

Fig. 1. The schematic illumination of Au/ZnO nanoparticle arrays deposition procedures.

10 μl of polystyrene nanosphere diluted solution onto a cleaned quartz substrate, which was inclined about 5° in a chamber with saturated humidity at a temperature of 35 °C, we successfully formed a homogenous, dense monolayer ordered nanosphere crystal mask. Then the substrate with the mask was mounted into a PLD system. A XeCl excimer laser (308 nm, 17 ns, 2 Hz) was alternately focused onto the high-purity targets of Au (99.99%) or Zn (99.99%) at a typically energy density 2 J/cm^2. The targets were mounted on a rotating holder, 45 mm from the substrates. Fig. 1 shows the schematic illumination of deposition procedures. Au was first deposited and then Zn, both for 10 min in vacuum at the pressure of about 1.0×10^{-5} mb at room temperature. The thicknesses of Au and Zn can be varied depending on the deposition time. After deposition, the nanosphere mask was completely removed by ultrasonication in chloroform, then the sample was annealed at 500 °C in pure O_2 atmosphere for 2 h, and finally the Au/ZnO nanoparticle arrays were obtained.

The nanostructure of the sample was characterized by atomic force microscopy (AFM; Digital Instruments, Nanoscope IIIa) in contact model. A VGESCALlab-5 X-ray photoelectron spectroscopy (XPS) with Mg Kα (1253.6 eV) exciting radiation was used to determine the Zn and Au chemical band. The binding energies were corrected with reference to the assumed value of 284.6 eV for the resulting C 1s line from the adsorbed hydrocarbon contaminant. The optical absorption of the sample was measured from 330 to 800 nm using a SpectraPro-500i spectrophotometer (Acton Research Corporation) at room temperature.

The third-order nonlinear susceptibility of the Au/ZnO nanoparticle arrays was determined by z-scan method [15]. The z-scan technique is a simple and effective tool for determining the nonlinear optical effects. It is used widely in material characterization because it provides not only the magnitudes but also the sign of the real and imaginary parts of $\chi^{(3)}$. When the measurement is performed without the aperture (open-aperture), the z-scan profile reveals the nonlinear absorption β alone. The normalized transmittance $T(z)$ could be written as [15]

$$T(z, s=1) = \sum_{m=0}^{\infty} \frac{[-q_0(z)]^m}{(m+1)^{3/2}} \quad \text{for} \quad |q_0| < 1 \tag{1}$$

where $q_0(z) = \beta I_0 L_{\text{eff}}/(1 + z^2/z_0^2)$, I_0 is the laser peak intensity, $L_{\text{eff}} = 1 - \exp(-\alpha L)/\alpha$ is the effective thickness of the films (L is the sample thickness) and z_0 is the diffraction length of the beam. While for the small aperture (closed-aperture) measurements, the transmittance is affected by both the nonlinear refraction and the nonlinear absorption. To extract the information of nonlinear refractive index n_2 from the z-scan curve, the closed-aperture transmittance was divided by the corresponding open-aperture data. Then the normalized transmittance $T(z)$ is given by [15]

$$T(z) \simeq 1 - \frac{4x}{(x^2+9)(x^2+1)} \Delta\Phi_0 \tag{2}$$

and

$$\Delta T_{p-v} \simeq 0.406(1-S)^{0.25} |\Delta\Phi_0| \quad \text{for} \quad |\Delta\Phi_0| \le \pi \tag{3}$$

where $\Delta\Phi_0$ is the on-axis phase shift at the focus, ΔT_{p-v} is the difference of transmittance between the normalized peak and valley. The linear transmittance of the far-field aperture, S, is defined as the ratio of the pulse energy passing through the aperture to the total energy.

A frequency-doubled Q-switched Nd:YAG laser at a wavelength of 532 nm with pulse width of 10 ns was used as the light source. The laser beam was focused onto the sample by a 150 mm focal length lens, leading to a measured beam waist of 30 μm and a pulse energy of 8.0 μJ at the focus. The on-axis transmitted beam energy, the reference beam energy, and the ratios of them were measured using an energy ratiometer (Rm 6600, Laser Probe Corp.) simultaneously. In order to reduce the possible thermal accumulative effect, the laser repetition rate was set to 1 Hz.

3. Results and discussion

Fig. 2 shows an AFM image of 5×5 μm^2 area of Au/ZnO nanoparticle arrays. The image exhibits a typical hexagonal patterned three-dimensional (3D) nanoparticle arrays consisting of triangular-shaped Au/ZnO nanoparticles. The in-plane particle diameter, defined as the perpendicular bisector of the equilateral triangle, is estimated to be about 45 nm. The average out-of-plane height of the nanoparticle arrays is about 18 nm. The height of pure Au nanoparticle arrays fabricated at the

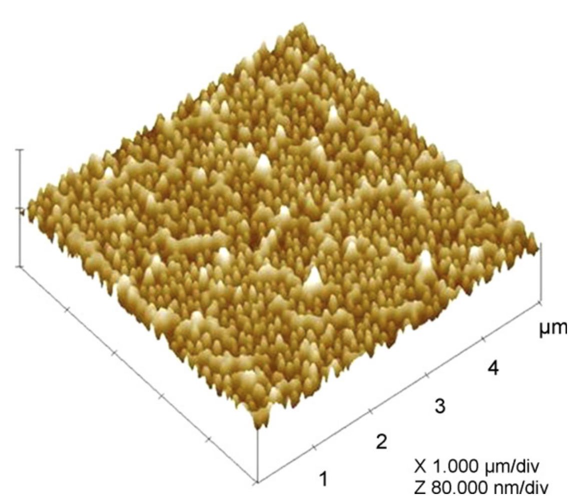

Fig. 2. AFM image of Au/ZnO nanoparticle arrays.

Please cite this article in press as: T. Ning, et al., Nonlinear optical properties of Au/ZnO nanoparticle arrays, Appl. Surf. Sci. (2007), doi:10.1016/j.apsusc.2007.07.195

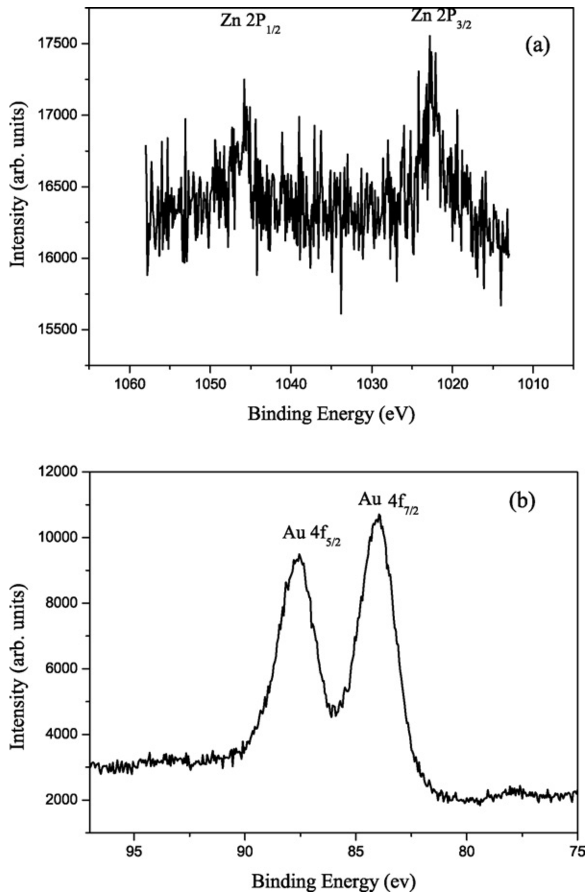

Fig. 3. Absorption spectrum of Au/ZnO nanoparticle arrays.

same condition was about 10 nm, so the thickness of the ZnO shell was estimated to be about 8 nm.

Fig. 3(a) exhibits Zn 2p XPS signal of the Au/ZnO nanoparticle arrays being bombarded by an argon ion (Ar^+) beam (2.5 kV, 20 μA) for 2 min. It is evident that the binding energy value of the Zn $2p_{3/2}$ peak is 1022.6 eV, indicating that Zn is in oxidized state and the signal of metallic Zn is too weak to be distinguished. Fig. 3(b) shows the XPS core-level spectra of Au 4f lines. The peaks at 84.0 and 87.7 eV are corresponding to Au $4f_{7/2}$ and $4f_{5/2}$, respectively, which indicate that the gold still kept metallic state in the composite arrays.

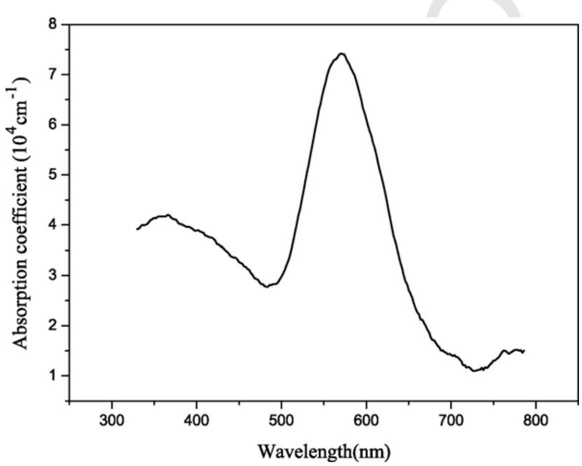

Fig. 4. (a) Zn 2p XPS spectrum of sample being etched by an Ar^+ ion beam (2.5 kV, 20 μA) for 2 min (b) Au 4f XPS spectrum of the sample, two peaks corresponding to Au $4f_{7/2}$ and $4f_{5/2}$.

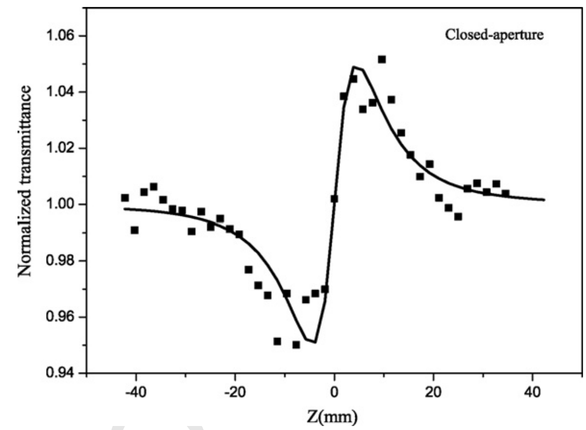

Fig. 5. z-Scan normalized transmittance with closed-aperture of Au/ZnO nanoparticle arrays. The solid curve is the theoretical fit to the data.

The absorption spectrum is shown in Fig. 4. The absorption peak due to the surface plasmon resonance of Au nanoparticles was observed around 570 nm. Compared with Au/ZnO composite film [7], the SPR of Au/ZnO nanoparticle arrays shifted to shorter wavelength. It is plausible that the shape and distribution of Au particles should be taken into consideration. The absorption peak near 364 nm arose from the exciton absorption of ZnO nanocrystallites. The absorption coefficient was calculated to be $5.2 \times 10^4\ cm^{-1}$ at 532 nm.

The typical curve of closed-aperture (CA) is shown in Fig. 5. The filled squares are the measured data, with each point corresponding to the average of 10 pulses. The solid line is the theoretical fit. The CA curve exhibits valley-to-peak configuration, indicating a positive value of the nonlinear refractive index n_2. Because the fused quartz substrate has a very small nonlinear optical response at 532 nm that was measured by the same z-scan setup, the large optical nonlinearity resulted from the Au/ZnO nanoparticle arrays. The result of open-aperture

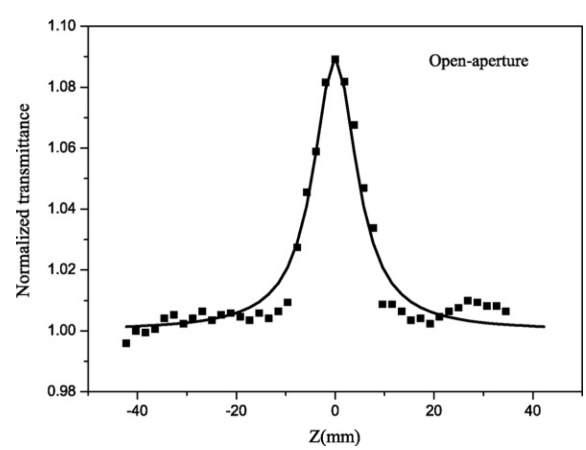

Fig. 6. z-Scan normalized transmittance with open-aperture of Au/ZnO nanoparticle arrays. The solid curve is the theoretical fit to the data.

Please cite this article in press as: T. Ning, et al., Nonlinear optical properties of Au/ZnO nanoparticle arrays, Appl. Surf. Sci. (2007), doi:10.1016/j.apsusc.2007.07.195

(OA) z-scan measurement of the sample is shown in Fig. 6. The OA curve exhibits a normalized transmittance peak, indicating the presence of nonlinear optical absorption saturation.

The data were analyzed using the procedures described by Sheik-Bahae et al. [15]. The calculated nonlinear refractive index, n_2, of the Au/ZnO nanoparticle arrays is 4.51×10^{-12} m^2/W and the real part of the third-order nonlinear optical susceptibility, Re $\chi^{(3)}$, is 1.15×10^{-6} esu, which is among the best values of some representative composite films such as Au:SiO_2 [4], Au:Al_2O_3[5], Au:$BaTiO_3$ [6] and Au:ZnO [7]. It is worth noting that the volume fraction of metal clusters in Au/ZnO nanoparticle arrays is only about 1.5% considering the air as the matrix, which is much lower than mentioned above. It is confirmed that the enhancement of the optical nonlinearity in the Au/ZnO nanoparticle arrays could be due to the strong local electric field near the triangular-shaped Au nanoparticles. Both the theoretical and experimental studies have demonstrated that the local fields near the particle surface is more intense for nonspherical particles than spherical ones, especially in the tips of a triangular particles with the high-curvature radius which tends to concentrate the electromagnetic field, and $|E|^2$ is as much as 10^4 times the incident field near the tips [16,17]. Meanwhile, the matrix of ZnO nanoparticles with strong nonlinear optical response also contributed to the large optical nonlinearity of the composite nanoparticle arrays [7].

The nonlinear absorption coefficient β (m/W) of the sample can be calculated to be -4.99×10^{-5} m/W. The calculated Im $\chi^{(3)}$ is -5.36×10^{-7} esu. The absolute value of $\chi^{(3)}$ was determined to 1.27×10^{-6} esu.

4. Conclusion

Nanocomposite particle arrays of Au/ZnO were fabricated on fused quartz substrate using nanosphere lithography. The structural characterization of the Au/ZnO nanoparticle arrays was investigated by atomic force microscopy. The AFM image of the sample illustrated a discrete triangular-shaped nanoparticle arrays with the height of the particles of 18 nm. XPS analysis indicated that the metallic Zn was oxidized to be ZnO, and Au still kept metallic state. The linear optical absorption spectrum showed SPR absorption of Au particles at 570 nm. The third-order optical nonlinearity of the sample was measured using z-scan technique at the wavelength of 532 nm with laser duration of 10 ns. The Re $\chi^{(3)}$ and Im $\chi^{(3)}$ of Au/ZnO were 1.15×10^{-6} and -5.36×10^{-7} esu, respectively. The results suggest that the Au/ZnO nanoparticle arrays have great potential application in the future optical devices.

Acknowledgements

This work was supported by the National Nature Science Foundation of China, Grant 10574157, and National Basic Research Program of China, No. 2006cb302900.

References

[1] D. Ricard, P. Roussignol, C. Flytzanis, Opt. Lett. 10 (1985) 511.
[2] D. Cotter, R.J. Manning, K.J. Blow, A.D. Ellis, A.E. Kelly, D. Nesset, I.D. Phillips, A.J. Poustie, D.C. Rogers, Science 286 (1999) 1523.
[3] V. Keibig, M. Vollmer, Optical Properties of Metal Clusters, Springer, Berlin, 1995.
[4] I. Tanahashi, Y. Manabe, T. Tohda, S. Sasaki, A. Nakamura, J. Appl. Phys. 79 (1996) 1244.
[5] H.B. Liao, R.F. Xiao, J.S. Fu, G.K.L. Wong, Appl. Phys. B 65 (1997) 673.
[6] W.T. Wang, Z.H. Chen, G. Yang, D.Y. Guan, G.Z. Yang, Y.L. Zhou, H.B. Lu, Appl. Phys. Lett. 83 (2003) 1983.
[7] H. Liao, W. Wen, G.K.L. Wong, G. Yang, Opt. Lett. 28 (2003) 1790.
[8] K.P. Yuen, M.F. Law, K.W. Yu, P. Sheng, Phys. Rev. E 56 (1997) 1322.
[9] K.P. Yuen, M.F. Law, K.W. Yu, P. Sheng, Opt. Commun. 148 (1998) 197.
[10] H.B. Liao, W. Wen, G.K.L. Wong, Appl. Phys. A 80 (2005) 861.
[11] D. Guan, Z. Chen, W. Wang, H. Lu, Y. Zhou, K.-j. Jin, G. Yang, J. Opt. Soc. Am. B 22 (2005) 1949.
[12] T.R. Jensen, G.C. Schatz, R.P. Van Duyne, J. Phys. Chem. B 103 (1999) 2394.
[13] H. Shen, B. Cheng, G. Lu, T. Ning, D. Guan, Y. Zhou, Z. Chen, Nanotechnology 17 (2006) 4274.
[14] W. Wang, Y. Wang, Z. Dai, Y. Sun, Y. Sun, Appl. Surf. Sci. 253 (2006) 4673.
[15] M. Sheik-Bahae, A.A. Said, T.H. Wei, D.J. Hagan, W. Van Stryland, IEEE J. Quantum Electron. 26 (1990) 760.
[16] T. Jensen, L. Kelly, A. Lazarides, G.C. Schatz, J. Clust. Sci. 10 (1999) 295.
[17] A.J. Haes, S. Zou, G.C. Schatz, R.P. Van Duyne, J. Phys. Chem. B 108 (2004) 6961.